Chapter

4D-MRI in Radiotherapy

Chunhao Wang and Fang-Fang Yin

Abstract

Four-dimensional (4D) imaging provides a useful estimation of tissue motion pattern and range for radiation therapy of moving targets. 4D-CT imaging has been a standard care of practice for stereotactic body radiation therapy of moving targets. Recently, 4D-MRI has become an emerging developmental area in radiotherapy. In comparison with 4D-CT imaging, 4D-MRI provides better spatial rendering of radiotherapy targets in abdominal and pelvis regions with improved visualization of soft tissue motion. Successful implementation of 4D-MRI requires an integration of optimized acquisition protocols, advanced image reconstruction techniques, and sufficient hardware capabilities. The proposed chapter intends to introduce basic theories, current research, development, and applications of 4D-MRI in radiotherapy.

Keywords: 4D-MRI, radiotherapy, image reconstruction, respiratory motion, motion artifacts

1. Introduction

The role of modern radiotherapy in cancer treatment is to irradiate target volumes that contain disease sites while sparing surrounding normal tissue. In classic 3D-based radiotherapy, treatment volumes are typically defined in **Figure 1(a)**. Gross tumor volume (GTV) contains the primary tumor or malignant tissue, and clinical target volume (CTV) contains GTV plus its surrounding tissue that may have subclinical disease that cannot be definitely revealed by medical imaging (though it is uncommon that CTV is identical to GTV in certain definitive radiotherapy). Planning target volume (PTV), which is often defined as treatment volume in a radiotherapy plan, is defined as CTV plus a margin that accounts for possible tissue displacement and patient positioning uncertainty within a treatment course that may last several weeks [1, 2]. This CTV to PTV margin can be called as setup margin. Depending on different treatment sites and disease stage, setup margin ranges from a few millimeters to 1–2 cm. However, in some radiotherapy treatment, the GTV volume is not stable: when treating tumors in lung, esophagus, and abdominal regions (liver, pancreas, etc.), tumors move under the effect of respiratory activity. Such target motion, referred as respiratory motion, has to be accounted in radiotherapy for effective therapeutic outcome. Thus, a large setup margin for PTV was proposed to account for possible respiratory motion. However, such simple solution has two problems: (1) amplitudes of respiratory motion vary among different individuals. Results of 1–2 mm up to 3 cm are commonly observed in clinic. A single large margin may not yield optimal treatment outcome for patients with extended/limited motion amplitudes [3]; and (2) a large setup margin may lead to unnecessary irradiation of normal tissue, which may substantially increase toxicity of radiotherapy. With the

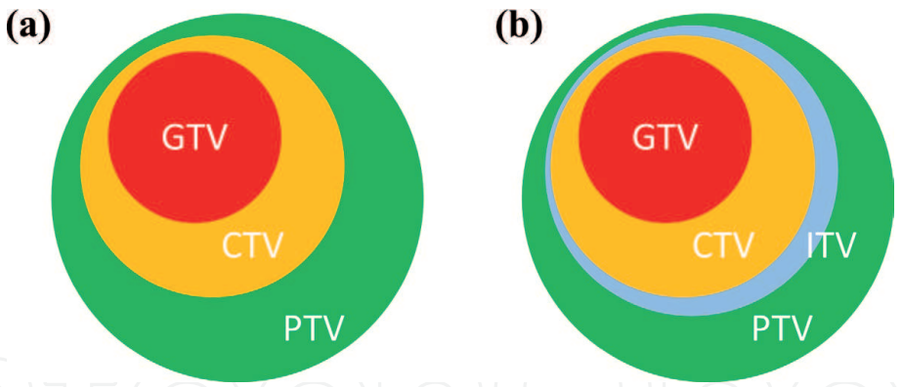

Figure 1.
Diagrams of volume definition in modern radiotherapy. (a) Definitions without consideration of target motion; (b) Definitions with ITV included to account for target motion.

current trend of stereotactic body radiotherapy (SBRT, also referred as stereotactic ablative body radiotherapy SABR) using very high radiation dose to treatment cancer in a few fractions, such big margin with large toxicity becomes unacceptable.

To account for aforementioned issue, dynamic imaging concept was proposed to capture individualized target motion pattern and amplitude. Such information can be used to define an internal target volume (ITV), which adds an internal margin to CTV that accounts for full possible motion range during radiotherapy (**Figure 1(b)**). This internal margin is determined on an individual basis during the initial treatment simulation. Compared to a generous setup margin, the added internal margin can maximize the therapeutic effect while reducing the irradiation to normal tissue [4, 5].

Prior to 4D imaging in radiotherapy, X-ray fluoroscopy imaging using C-arm device was the early effort to determine individualized internal margin [6]. The lack of volumetric information in this approach cannot capture the potential motion pattern heterogeneity. Since CT is the dominant modality for radiotherapy with its irreplaceable tissue electron density information required by radiation dose calculation, proposed in the 2000s, 4D-CT has become the standard imaging technique of treatment moving target [7]. **Figure 2** shows a diagram of 4D-CT. For a simple description, 4D-CT samples projections repetitively at a couch position for at least one respiratory cycle before moving to the next imaging position. With synchronized respiratory cycle information, all projections are retrospectively sorted into

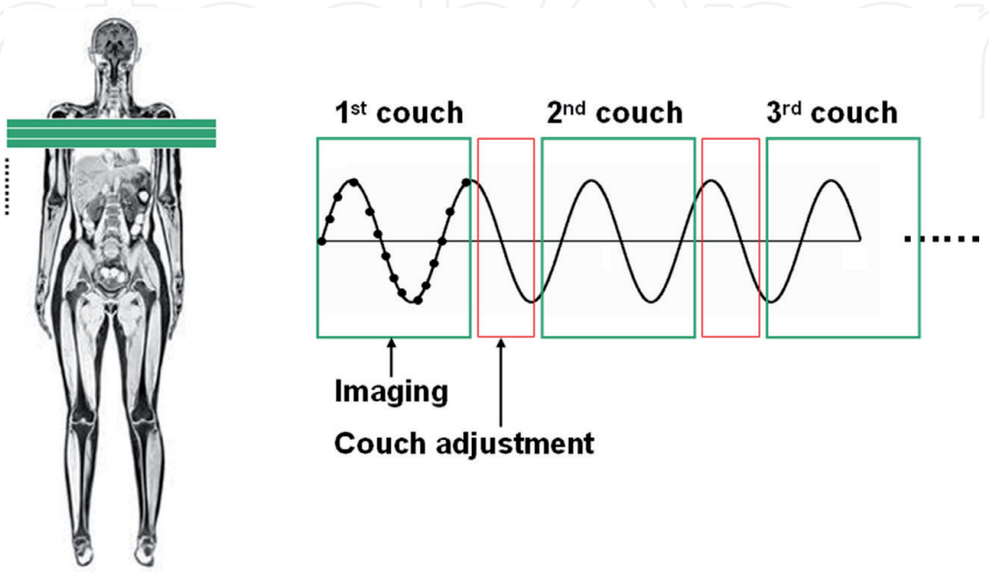

Figure 2.
A simple diagram of 4D-CT implementation.

different phase bins (typically 10) that consists of an averaged respiratory cycle derived from the whole scan period [8]. The respiratory cycle information is usually derived by recording 2D trajectories of external surrogates, such as inferred reflection markers and pneumatic bellows [9, 10]. As a result, multiple 3D CT volumes from different phase volumes are reconstructed. By delineating CTV volumes at each 3D volume, ITV can be generated as a union of CTVs from all phases with a possible small margin for positioning uncertainty.

Despite of its popularity, 4D-CT has a few problems: (1) when patient's breath becomes irregular in terms of amplitude and period length, abrupt changes in projections may lead to motion-induced artifacts in the reconstructed phase volumes. **Figure 3** shows a reconstructed phase volume in 4D-CT. The diaphragm boundary discontinuity with a ghost displacement indicated by red arrow is a typical rendering of motion artifacts in 4D-CT; (2) although trajectories of external surrogates and internal organs are correlated [11], potential hysteresis between the two trajectories may impact overall treatment accuracy [12]; and (3) 4D-CT requires extended scan time and leads to increased imaging radiation dose as a potential patient health risk.

In addition to 4D-CT, ultrasound has been utilized for motion assessment in radiotherapy because of its fast imaging time and relatively simple implementation. Earlier application of ultrasound focused at localizing displaced prostate radiotherapy volume through transrectal imaging [13]. To image respiratory motion, previous work reported its use for upper abdominal radiotherapy. In addition to assess motion at simulation, same imaging strategy can be deployed at each treatment fraction for real-time verification [14, 15]. However, motion assessment using ultrasound sometime can only be achieved by indirect measurement of a nearby landmark instead of target volume [16]. The generally poor visualization capability of ultrasound limits its utilization in the current practice of radiotherapy.

Following the increased utilization of MRI in radiotherapy, 4D-MRI has become a popular area in image-guided radiotherapy (IGRT) after the birth of 4D-CT. Generally, MRI has excellent soft-tissue contrast with zero radiation hazard in comparison to 4D-CT. 4D-MRI is thus highly desirable in the radiotherapy workflow. In the last decade, many works have been done for the development of 4D-MRI. At present, however, there is no fully established 4D-MRI technique by major vendors in radiotherapy clinic. Implementation of 4D-MRI in clinic is still at investigational stage due to excessive technical involvement. Nevertheless, current results of 4D-MRI application showed its promising value in the era of IGRT [17].

In the following section, we will introduce 4D-MRI basic theories and current technologies and discuss emerging topics in 4D-MRI research and development. Radiotherapy application of 4D-MRI will be discussed based on our clinical experience in another section.

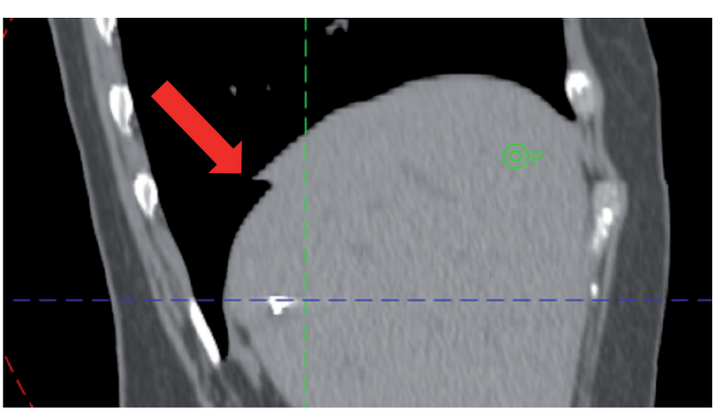

Figure 3.
An example of motion artifacts in 4D-CT.

2. 4D-MRI: basic theories and technologies

In this section, we first describe the brief history of 4D-MRI debut and then discuss basic theories and implementation technologies of current 4D-MRI methods. Frontier research topics in 4D-MRI are introduced in the rear part in this section.

2.1 Fast imaging: early effort

Earliest effort for MRI-based motion quantification focused on 2D-based cine imaging, i.e., continuously acquire images at a fixed 2D coordinate frame. The acquired 2D images could be stacked as a movie that described target motion. This requires fast imaging sequences to achieve high frame rates. Several approaches were employed. Koch et al. first used gradient echo technique in lung motion imaging [18]. Shimizu et al. imaged liver tumor motion with multiple T1-weighted gradient slices [19]. Kirilova et al. used T2-weighted single shot fast spin echo sequence for liver tumor position tracking [20]. A handful of works adopted balanced steady-state free precession (bSSFP) imaging on three orthogonal planes for tumor as well as diaphragm motion tracking [21, 22]. The reported frame rate using bSSFP could be up to 10 frames per second.

The obvious drawback of 2D cine imaging is the deficiency of volumetric motion capture, which is critical when motion pattern is heterogeneous within the imaging region of interest (ROI). Repetitive 3D volume acquisition (i.e., real-time 4D-MRI) was then investigated since it yielded truly real-time volumetric imaging without additional post-processing. This approach is usually accomplished with parallel imaging with a trade of image quality. Blackall et al. used fast file echo with echo planar imaging (FFE-EPI) for real-time 4D-MRI implementation for lung RT planning [23]. In spite of its reported high temporal resolution (up to 330 ms/frame), the acquired image showed considerably less vessel structure details within the lung. Dinkel et al. implemented TREAT sequence, a 3D time-resolved echo shared gradient echo sequence with parallel imaging [24]. This technique achieved a frame rate of 1400 ms/frame covering a large field of view (FOV) (400 × 400 × 300 mm) with a relatively low spatial resolution (voxel size 3.1 × 3.1 × 4 mm). Tryggestad et al. reported their real-time 4D-MRI protocol with frame rate 1000 ms/frame at the cost of lower signal-to-noise ratio (SNR) and intrascan motion [25]. However, these works did not achieve high temporal resolution and acceptable spatial resolution at the same time. Since a typical human's breathing cycle period is about 3–5 seconds, high temporal resolution <500 ms/frame is desired for multiphase reconstruction. In addition, high spatial resolution at the level of 1 mm isotropic voxel size might be necessary for small size SBRT target in lung/liver treatment, which could be 1 cc or less. Currently available MR scanner capabilities limit further improvement of real-time 4D-MRI.

2.2 Retrospective sorting: 2D-based

Retrospective sorting has been the mainstream technique for 4D-MRI reconstruction. Similar to the 4D-CT implementation, retrospective sorting in 4D-MRI records a motion surrogate's trajectory during the scan. Acquisition data are sorted into different bins based on the amplitude/phase information of the surrogate trajectory. To date, retrospective sorting with multislice dynamic 2D acquisition (2D-based sorting) is commonly reported for clinical and preclinical investigations. In short, 2D MRI image slices at interleaved slice locations were sorted accordingly before 3D volume stacking. By theory, this strategy can achieve high spatial resolution while maintaining high in-plane spatial resolution. On the other hand, retrospective sorting requires intensive image post-processing offline with high software demand.

So far, several works of 2D-based sorting techniques have been reported with different motion surrogate selection and image acquisition sequence. von Siebenthal et al. invented a navigator-based sorting method. In this method, navigator slices were acquired at a fixed location, interleaved with slice locations that were sequentially stepped through the imaging volume. 2D images were acquired using 2D bSSFP sequence repetitively for nearly 1 hour. Image sorting was carried based on navigator slice similarity using a cost function that combines directional shifts of image registration [26]. This sophisticated scheme achieve 180 ms/frame temporal resolution and 1.8 × 1.8 mm in-plane resolution, but the navigator acquisition prolonged total scan time and did not guarantee measurement reproducibility.

Remmert et al. investigated the feasibility of using respiratory surrogate. A rapid imaging sequence using 2D fast low-angle shot (FLASH) with generalized auto-calibrating partially parallel acquisition (GRAPPA) was adopted on Cartesian grid. Respiratory surrogate was extracted as the positioning of the piston rod of the imaged dynamic porcine lung phantom [27]. The results demonstrated the feasibility of respiratory surrogate sorting. Hu et al. implemented a respiratory-triggered 4D-MRI reconstruction. The respiratory amplitude was derived from a turbo spin echo sequence, and 2D image acquisition was achieved by T2-weighted EPI [28]. The in vivo demonstration of this technique in healthy volunteers successfully reconstructed four phase volumes.

Other surrogates are also proposed for convenient sorting implementation. Cai et al. proposed a sorting surrogate based on body area (BA), which was defined as the area inside the binary mask of body contour from 2D fast steady-state acquisition (FIESTA). The surrogate trajectory was determined by excluding the low-frequency change of BA as subject anatomic change [29]. Tryggestad et al. integrated signals from Physiologic Monitoring Unit (PMU) by Siemens for retrospective sorting. This PMU signal was derived from a pneumatic device attached to the subject's upper abdomen. Acquired at 50 Hz sampling rate, the PMU signal was synchronized with 2D repetitive acquisition [25].

In spite of its popularity, 2D-based sorting methods suffer from two major problems: (1) large slice thickness (typically 5–10 mm) may not be sufficient to quantify target motion when the target is small, and the reconstructed volume may not look like continuous on slice direction; and (2) the reconstructed images tend to have stitch motion artifacts similar to those in 4D-CT. **Figure 4** shows an example of stitch motion artifacts. This resorting artifact of radiant rays is caused by unpredicted motion change during image acquisition.

2.3 Retrospective sorting: 3D-based

3D-based retrospective sorting has gained its attention with advances of both imaging hardware and software technologies. Similar to 2D-based equivalent, 3D-based retrospective sorting requires motion surrogate recording synchronized with data acquisition. The most distinguished feature of 3D-based sorting is that raw k-space acquisitions, rather than 2D image data in real space, are sorted into different phase volume bins. Image reconstruction in 3D fashion (but could also be done in 2D) has to be performed after retrospective sorting. Image quality can be improved with advanced image reconstruction technique with possible isotropic voxel size. Generally, 3D-based retrospective sorting requires more sophisticated data processing algorithms and more demanding hardware manipulation. Nevertheless, 3D-based retrospective sorting has become the selection by most recent 4D-MRI developments.

In 2008, Tokuda et al. proposed an early trial of 3D-based retrospective sorting. The acquired k-space echo was filled into multiple assigned bins based on

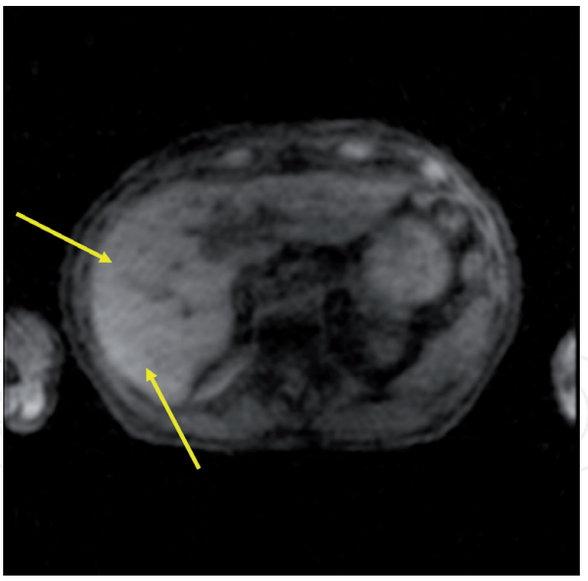

Figure 4.
An example of stitch motion artifacts in reconstructed 4D-MRI. This image was reconstructed from computer simulation instead of human subject imaging.

amplitude ranges of respiratory surrogate, which was implemented by a navigator echo acquired at a configurable sampling rate [30]. In a patient study, 4D volumes were successfully reconstructed using 10.5 min acquisition time with compromised image quality compared with breath-hold (BH) 3D acquisitions.

In the last several years, several representative works with 3D-based sorting have been reported as most recent advances in 4D-MRI. Deng et al. utilized a continuous spoiled gradient echo sequence with 3D radial trajectory for fast volumetric acquisition [31]. Respiratory surrogate was derived as "self-gating" (SG) measurement, which was 1D Fourier transform of SG acquisition lines through the k-space center (k_z direction). Acquisitions were retrospectively sorted into ten phase volumes using phase percentage information on surrogate trajectory, and image reconstruction was carried out with a conjugate-gradient sensitivity encoding (CG-SENSE) with self-sensitivity calibration [32].

Similarly, Feng et al. proposed a 4D-MRI framework XD-GRASP (extra-dimension golden-angle radial sparse parallel) technique, which included 3D radial-based acquisition trajectory and surrogate with SG [33]. Principal component analysis (PCA) could be used on SG surrogate to separate cardiac motion or MR contrast uptake from respiratory motion. Each 3D volume was iteratively reconstructed on radial grid.

Acquisition on Cartesian grid has also been reported. Han et al. invented a rotating 3D Cartesian k-space recording method (ROCK) for 4D-MRI acquisition [34]. This method simulated a quasispiral acquisition trajectory with varying sampling densities on radial direction. Balanced SSFP sequence was chosen for its improved SNR over gradient recalled echo technique, and amplitude-based sorting was based on SG motion surrogate. Wang et al. also implemented a sparse Cartesian-based acquisition trajectory simulating a multi-ray profile regulated by golden-ratio angular increment [35].

2.4 Discussion: technical factors in 4D-MRI

As a summary of current 4D-MRI works (with a focus on 3D-based retrospective sorting approach), we hereby discuss a few key technical factors that one may need to consider for developing a 4D-MRI method:

2.4.1 Acquisition protocol

K-space acquisition can be realized by different techniques since retrospective sorting does not directly depend on data acquisition scheme. Both radial-based and Cartesian-based trajectories are valid for acquisition. Since radial-based trajectories have higher sampling density near k-space center (low-frequency component) in their nature, they might be preferred for fast 3D acquisition. Golden-ratio means or its equivalent technologies are commonly used for 4D-MRI since the azimuthal increments are relatively constant after volume sorting [36–38]. However, radial-based trajectories may lead to severe motion artifacts after retrospective sorting when the subject's motion is irregular [34]. Cartesian-based trajectories could simulate k-space central/peripheral sampling weights in radial-trajectories and might be easier for image reconstruction without data regridding. Nevertheless, both approaches require extensive hardware/software editing that most clinical MR units may not be fully ready for.

To implement SG, low-frequency component in k-space has to be sampled repeatedly during the total acquisition time. As discussed above, SG can be derived as 1D projection on k_z direction through k-space center. SG signal can capture displacement on superior-inferior (SI) direction that is sensitive to respiratory motion [39]. SG can also be derived as phase shift measurement of 0-frequency (DC) point at k-space center [35]. It has to be pointed out that k-space center does not have to be sampled periodically as long as the sampling intervals are known. Since the human breath is mostly modeled as sinusoid waveform, it is more straightforward to sample k-space center at certain rhythms.

2.4.2 Retrospective sorting practice

In retrospective sorting, data binning can use either surrogate's amplitude or phase percentage (temporal location within a breath cycle) information. Both approaches are valid in both 4D-MRI and 4D-CT. However, when the subject's breathing is not regular, potential error could be made in retrospective sorting [40, 41]. In clinical practice, intrascan variation of both breathing amplitude and period is commonly seen. There is no established theory regarding variation theory, but breathing period is subject to more change when the scan time is long for pulmonary function compromised subjects. Drastic change of surrogate amplitude, however, is usually caused by random event such as cough.

To reduce irregularity-induced data divergence, a straightforward way is to employ external motion management devices as in 4D-CT imaging, such as abdominal compression and body vacuum bag. However, such devices can be cumbersome for MR imaging protocols.

During retrospective sorting, one determines certain threshold values and excludes data acquisitions when surrogate trajectory is out of range [29]. In spite of its simplicity, this approach may reduce data utility when the subject's breathing is irregular, which may further lead to undersampling artifacts in the reconstructed images. A soft-gating approach has been reported for amplitude-based on a Gaussian weighting function with its Full width at half maximum (FWHM) determined as a function of surrogate motion range [34]. This approach can improve data utilization with improved SNR in the reconstructed images [42, 43].

Wang et al. designed a spatiotemporal index (STI) as a quadratic sum of amplitude and phase discrepancies in retrospective sorting [35]. Each acquisition can be used for reconstructing multiple phase volumes when discrepancy criteria are met. In combination with the selected acquisition trajectory, such criteria were designed as tight rules near k-space center and loose rules near k-space periphery to further improve data utilization.

2.4.3 Image reconstruction

Image reconstruction has become a focused topic in 4D-MRI because of sparse k-space data after 3D-based retrospective sorting. With the advent of compressed sensing, i.e., extract compressible signal from undersampled data, many iterative MR reconstruction algorithms have been successfully developed [44–46]. In the specific 4D-MRI reconstruction, L1-norm (total variation [47]), L2-norm (total generalized variation, TGV [48]; Tikhonov regularization [49]), and wavelet (Daubechies [50]) regularization algorithms have been utilized. Detailed mathematics of these algorithms go beyond the scope of this discussion.

A unique feature of 4D-MRI reconstruction is the potential implementation of spatiotemporal constrained reconstruction. Because of averaging nature in retrospective sorting, motion continuity is usually guaranteed after reconstructing each phase volume as an independent 3D volume. A possible improvement is view sharing, which enable the use of same data in multiple volumes. Such technique has been widely used in dynamic MRI imaging for pharmacokinetics study [51, 52]. Because of motion sensitivity of low-frequency k-space component, view sharing of high-frequency component in combination with iterative reconstruction is a viable solution [35]. Temporal constraint can also be explicitly written as penalty terms in reconstruction. Total variation representation of finite motion differences has been adopted [33, 34].

2.5 Emerging topics in 4D-MRI research

Trends in 4D-MRI research have been following evolving technologies in radiation oncology. The most relative topic is to use deformable image registration (DIR) to model anatomic motion during respiratory cycles. A detailed description of DIR cannot be included in this section; for a short discussion, DIR tries to wrap one image to another one with much more transform degrees that are different across the ROI instead of 6 rigid transform degrees. A registration is represented by a deformation vector field (DVF) in the same size as the source image, which points each single voxel in source image to its destination in the coordinate system of target image. DIR has been used in radiotherapy for time-series image registration, image outcome for treatment assessment, and dose wrapping for adaptive therapy [53].

In 4D-MRI, the motion-induced anatomic change can be seen as a deformation process. Each phase volume (2D or 3D) is a deformation from a standard reference volume. This reference volume can be a stable phase volume in 4D series (such as end-of-exhalation (EOE) phase) or a breath-hold (BH) volume. Thus, respiratory motion can be described by a series of DVFs derived from DIR. This enables the motion information transfer to recreate respiratory motion derived from one MR contrast to another one [54].

Recently, Harris et al. and Stemkens et al. proposed their similar approaches of 4D-MRI reconstruction based on DIR manipulation and a priori patient-specific motion model [55, 56]. When a 4D-MRI series for a patient is available, a series of DVFs could be generated by DIR. Principal component analysis (PCA) was used to decompose this DVF series into three principle components (PCs). Any future motion imaging could be seen as a simple weighted sum of these three PCs. To derive the three weighting coefficients, the acquisition could be done rapidly by single or multislice 2D acquisition, and the coefficients were solved as a minimization problem based on the similarity of the reconstructed 4D-MRI series at fixed position(s) with 2D acquisition(s) [57]. Because of rapid 2D acquisition, this method could generate volumetric images in cine fashion up to 20 frames/s [57]. Harris et al. also reported that such rapid 2D acquisition can be done by planar KV fluoro images which are widely available on modern radiation linear accelerators

(LINAC) [58, 59]. This point attracts the attention since MR-based radiotherapy treatment guidance can be realized on current radiotherapy platform.

It is crucial to ensure the DIR accuracy when generating the DVF. Li et al. reported their time-resolved 4D-MRI (TR-4DMRI) method with improved DIR reconstruction. Based on the a priori motion information, a pseudo demon force was introduced and applied to the coarse volumetric alignment. The fine-tuning of DIR was performed at multiple resolutions by demon forces [60]. This method was argued with better handle of large anatomy deformation during possible irregular breath. Digital phantom results showed that this technique successfully reconstructed fast 4D series and identified some questionable cases without missing true negative.

The wave of artificial intelligence (AI) in medicine (specifically in radiation oncology imaging) has enlightened many sparkling ideas in medical imaging research [61]. Together with the use of AI in pattern recognition from large-scale data, the currently required patient-specific motion pattern can be potentially derived from population results. Thus, 4D-MRI based on DIR modeling may become the focus of 4D-MRI research in the next decade.

3. 4D-MRI: clinical application

Although 4D-MRI has been demonstrated with great potential of anatomic motion quantification, its application in clinic is still premature for standard practice. Nevertheless, a few works have reported 4D-MRI's values in radiotherapy clinic. In this section, we discuss possible clinical applications of 4D-MRI in radiotherapy.

3.1 Radiotherapy target delineation

Similar to the 4D-CT application, 4D-MRI provides motion direction and quantified motion range information for ITV generation at the same level of accuracy as 4D-CT [62]. Because of superior soft tissue contrast, 4D-MRI may better illustrate ITV definition with finer anatomical detail boundaries.

Figure 5 shows an example of 4D-MRI-based ITV delineation for liver SBRT in our clinic. This case was about liver mets from breast cancer, and the prescription was 16Gy × 3 fractions. 4D-MRI was acquired by bSSFP sequence with 2D-based retrospective sorting [29]. Interslice distance was 5 mm. A total of 10 phase volumes (0, 10, … 90%) were reconstructed. GTV was contoured in each phase volume as shown by red contours in five representative phase volumes in **Figure 5**. The reference frame of 4D-MRI was registered to the planning CT volume by rigid transform. ITV-MRI, the union of 10 GTVs from 4D-MRI, was mapped to the planning CT as illustrated. The final ITV for this case was adjusted by our radiation oncologist to combine information from both MRI and CT studies.

3.2 Onboard treatment guidance

Since 2010, MR-guided radiotherapy units have become commercially available. The integrated onboard MR imaging capability can provide potentially improved patient positioning accuracy with affluent soft tissue details. In addition, intra-treatment imaging during radiation enables image-based treatment gating, which could reduce margin size for PTV definition with potentially reduced normal tissue toxicity [63]. Currently, both low-field-strength (0.35 T) unit (ViewRay, Oakwood Village, Ohio) and high-field-strength (1.5 T) unit (Elekta AB, Stockholm, Sweden) have started treating patient.

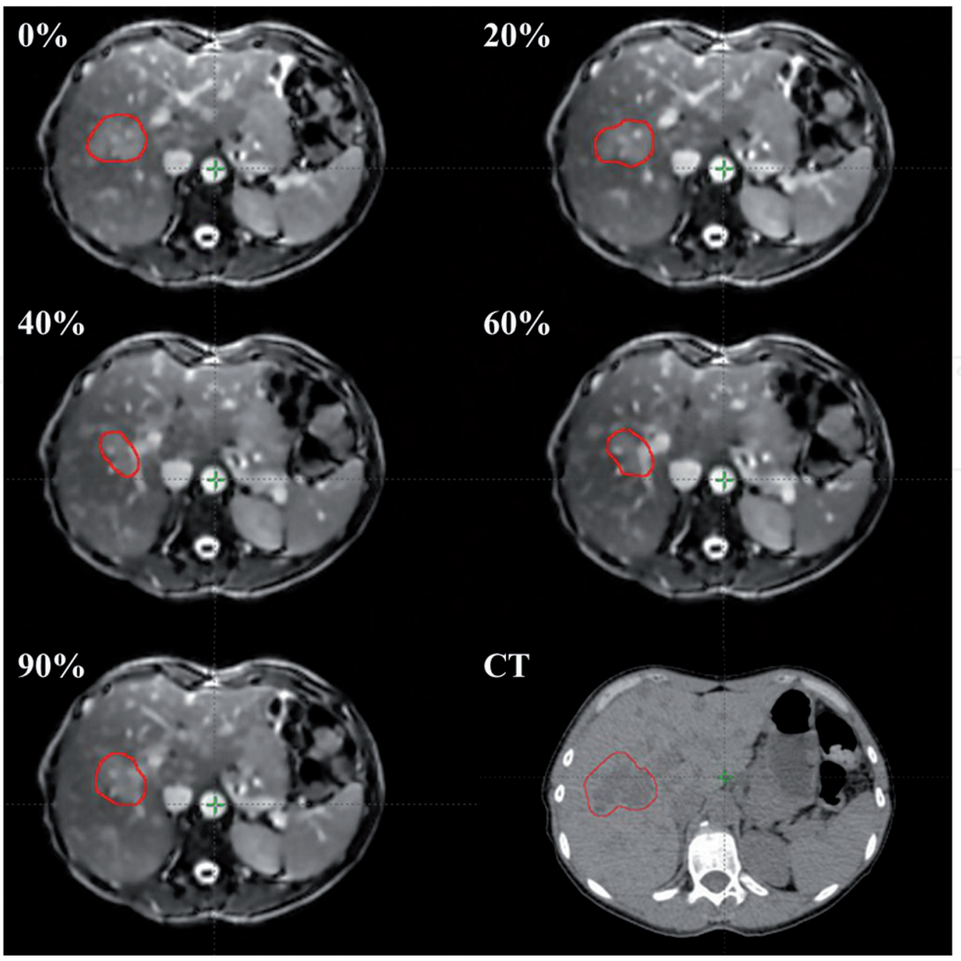

Figure 5.
A clinical example of 4D-MRI in liver SBRT target delineation.

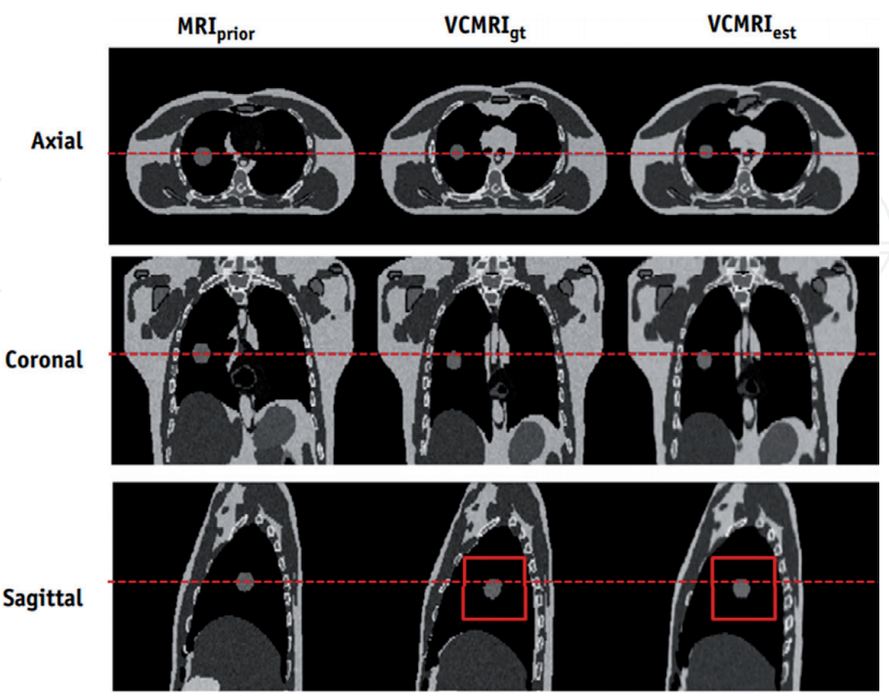

Figure 6.
VC-MRI for onboard MR imaging accuracy simulation. MRI$_{prior}$, reference EOE volume in pre-treatment 4D-MRI simulation; VCMRI$_{gt}$, ground truth EOI volume at treatment day for onboard match; and VCMRI$_{est}$, estimated EOI volume from the proposed VC-MRI approach.

Onboard image guidance on MR-guided radiotherapy units are implemented by 2D imaging on orthogonal views. Volumetric imaging, though technically feasible, are not realistic because of long imaging time. At this moment, no in vivo implementation of onboard 4D-MRI guidance has been reported. Nevertheless, a few works have tried to demonstrate its feasibility. Harris et al. used digital XCAT phantom simulation to examine their VC-MRI technique for onboard patient positioning accuracy [56]. As shown in **Figure 6**, the estimated VC-MRI volume at end-of-inhalation (EOI) phase (third column) was accurate when comparing to the ground truth volume (second column). The reported target center-of-mass-shift (COMS) was about 1 mm or less on SI direction in most simulation scenarios.

Han et al. implemented their ROCK 4D-MRI technique on their 0.35 T-MR-guided radiotherapy unit [64]. Seven patients with abdominal tumors were imaged with both ROCK 4D-MRI and 2D-cine (reference) techniques. Because of relatively long imaging time (~10 min) in ROCK, image acquisition was performed after treatment as feasibility studies. They reported that when compared with reference 2D-cine results, motion quantification in 4D-MRI was about 1 mm different on SI direction. 3D anatomical details were successfully rendered without motion artifacts for onboard imaging. Optimistically speaking, 4D-MRI for pre-treatment patient positioning could become available in the next decade with novel 4D-MRI methods and improved hardware developments.

Author details

Chunhao Wang* and Fang-Fang Yin
Department of Radiation Oncology, Duke University Medical Center, Durham, NC, United States

*Address all correspondence to: chunhao.wang@duke.edu

References

[1] Khan FM, Gibbons JP. Khan's the Physics of Radiation Therapy. Baltimore, MD: Lippincott Williams & Wilkins; 2014

[2] Landberg T, Chauaudra J, Dobbs H. Prescribing, Recording and Reporting Photon Beam Therapy: ICRU Report 50. Maryland, USA: International Commission on Radiotherapy Units and Measurements; 1993

[3] Ozhasoglu C, Murphy MJ. Issues in respiratory motion compensation during external-beam radiotherapy. International Journal of Radiation Oncology, Biology, Physics. 2002;**52**(5):1389-1399

[4] Stroom JC, Heijmen BJ. Geometrical uncertainties, radiotherapy planning margins, and the ICRU-62 report. Radiotherapy and Oncology. 2002;**64**(1):75-83

[5] Jin J-Y et al. A technique of using gated-CT images to determine internal target volume (ITV) for fractionated stereotactic lung radiotherapy. Radiotherapy and Oncology. 2006;**78**(2):177-184

[6] Siewerdsen J et al. Multimode C-arm fluoroscopy, tomosynthesis, and cone-beam CT for image-guided interventions: From proof of principle to patient protocols. In: Medical Imaging 2007: Physics of Medical Imaging. San Diego, CA: International Society for Optics and Photonics; 2007

[7] Low DA et al. A method for the reconstruction of four-dimensional synchronized CT scans acquired during free breathing. Medical Physics. 2003;**30**(6):1254-1263

[8] Pan T et al. 4D-CT imaging of a volume influenced by respiratory motion on multi-slice CT. Medical Physics. 2004;**31**(2):333-340

[9] Glide-Hurst CK et al. Evaluation of two synchronized external surrogates for 4D CT sorting. Journal of Applied Clinical Medical Physics. 2013;**14**(6):117-132

[10] Quirk S, Becker N, Smith W. External respiratory motion analysis and statistics for patients and volunteers. Journal of Applied Clinical Medical Physics. 2013;**14**(2):90-101

[11] Hoisak JD et al. Correlation of lung tumor motion with external surrogate indicators of respiration. International Journal of Radiation Oncology, Biology, Physics. 2004;**60**(4):1298-1306

[12] Ruan D et al. Inference of hysteretic respiratory tumor motion from external surrogates: A state augmentation approach. Physics in Medicine & Biology. 2008;**53**(11):2923

[13] Lattanzi J et al. Ultrasound-based stereotactic guidance of precision conformal external beam radiation therapy in clinically localized prostate cancer. Urology. 2000;**55**(1):73-78

[14] Fuss M et al. Daily ultrasound-based image-guided targeting for radiotherapy of upper abdominal malignancies. International Journal of Radiation Oncology, Biology, Physics. 2004;**59**(4):1245-1256

[15] O'shea T, Bamber J, Harris E. MO-DE-210-05: Improved accuracy of liver feature motion estimation in B-Mode ultrasound for image-guided radiation therapy. Medical Physics. 2015;**42**(6Part28):3560-3560

[16] Mason SA et al. Towards ultrasound-guided adaptive radiotherapy for cervical cancer:

Evaluation of Elekta's semiautomated uterine segmentation method on 3D ultrasound images. Medical Physics. 2017;**44**(7):3630-3638

[17] Dawson LA, Sharpe MB. Image-guided radiotherapy: Rationale, benefits, and limitations. The Lancet Oncology. 2006;**7**(10):848-858

[18] Koch N et al. Evaluation of internal lung motion for respiratory-gated radiotherapy using MRI: Part I—correlating internal lung motion with skin fiducial motion. International Journal of Radiation Oncology, Biology, Physics. 2004;**60**(5):1459-1472

[19] Shimizu S et al. High-speed magnetic resonance imaging for four-dimensional treatment planning of conformal radiotherapy of moving body tumors1. International Journal of Radiation Oncology, Biology, Physics. 2000;**48**(2):471-474

[20] Kirilova A et al. Three-dimensional motion of liver tumors using cine-magnetic resonance imaging. International Journal of Radiation Oncology, Biology, Physics. 2008;**71**(4):1189-1195

[21] Feng M et al. Characterization of pancreatic tumor motion using cine MRI: Surrogates for tumor position should be used with caution. International Journal of Radiation Oncology, Biology, Physics. 2009;**74**(3):884-891

[22] Cai J et al. Evaluation of the reproducibility of lung motion probability distribution function (PDF) using dynamic MRI. Physics in Medicine & Biology. 2006;**52**(2):365

[23] Blackall J et al. MRI-based measurements of respiratory motion variability and assessment of imaging strategies for radiotherapy planning. Physics in Medicine & Biology. 2006;**51**(17):4147

[24] Dinkel J et al. 4D-MRI analysis of lung tumor motion in patients with hemidiaphragmatic paralysis. Radiotherapy and Oncology. 2009;**91**(3):449-454

[25] Tryggestad E et al. Respiration-based sorting of dynamic MRI to derive representative 4D-MRI for radiotherapy planning. Medical Physics. 2013;**40**(5):051909

[26] von Siebenthal M et al. 4D MR imaging of respiratory organ motion and its variability. Physics in Medicine & Biology. 2007;**52**(6):1547

[27] Remmert G et al. Four-dimensional magnetic resonance imaging for the determination of tumour movement and its evaluation using a dynamic porcine lung phantom. Physics in Medicine & Biology. 2007;**52**(18):N401

[28] Hu Y et al. Respiratory amplitude guided 4-dimensional magnetic resonance imaging. International Journal of Radiation Oncology Biology Physics. 2013;**86**(1):198-204

[29] Cai J et al. Four-dimensional magnetic resonance imaging (4D-MRI) using image-based respiratory surrogate: A feasibility study. Medical Physics. 2011;**38**(12):6384-6394

[30] Tokuda J et al. Adaptive 4D MR imaging using navigator-based respiratory signal for MRI-guided therapy. Magnetic Resonance in Medicine. 2008;**59**(5):1051-1061

[31] Deng Z et al. Four-dimensional MRI using three-dimensional radial sampling with respiratory self-gating to characterize temporal phase-resolved respiratory motion in the abdomen. Magnetic Resonance in Medicine. 2016;**75**(4):1574-1585

[32] Pang J et al. Accelerated whole-heart coronary MRA using motion-corrected

sensitivity encoding with three-dimensional projection reconstruction. Magnetic Resonance in Medicine. 2015;**73**(1):284-291

[33] Feng L et al. XD-GRASP: Golden-angle radial MRI with reconstruction of extra motion-state dimensions using compressed sensing. Magnetic Resonance in Medicine. 2016;**75**(2):775-788

[34] Han F et al. Respiratory motion-resolved, self-gated 4D-MRI using rotating cartesian k-space (ROCK). Medical Physics. 2017;**44**(4):1359-1368

[35] Wang C et al. A spatiotemporal-constrained sorting method for motion-robust 4D-MRI: A feasibility study. International Journal of Radiation Oncology, Biology, Physics. 2018;**103**(3):758-766

[36] Kazantsev IG, Matej S, Lewitt RM. Optimal ordering of projections using permutation matrices and angles between projection subspaces. Electronic Notes in Discrete Mathematics. 2005;**20**:205-216

[37] Tsai CM, Nishimura DG. Reduced aliasing artifacts using variable-density k-space sampling trajectories. Magnetic Resonance in Medicine. 2000;**43**(3):452-458

[38] Chan RW et al. Temporal stability of adaptive 3D radial MRI using multidimensional golden means. Magnetic Resonance in Medicine. 2009;**61**(2):354-363

[39] Pang J et al. ECG and navigator-free four-dimensional whole-heart coronary MRA for simultaneous visualization of cardiac anatomy and function. Magnetic Resonance in Medicine. 2014;**72**(5):1208-1217

[40] Jiang SB. Technical aspects of image-guided respiration-gated radiation therapy. Medical Dosimetry. 2006;**31**(2):141-151

[41] Lu W et al. A comparison between amplitude sorting and phase-angle sorting using external respiratory measurement for 4D CT. Medical Physics. 2006;**33**(8):2964-2974

[42] Cheng JY et al. Free-breathing pediatric MRI with nonrigid motion correction and acceleration. Journal of Magnetic Resonance Imaging. 2015;**42**(2):407-420

[43] Uecker M et al. ESPIRiT—an eigenvalue approach to autocalibrating parallel MRI: Where SENSE meets GRAPPA. Magnetic Resonance in Medicine. 2014;**71**(3):990-1001

[44] Gamper U, Boesiger P, Kozerke S. Compressed sensing in dynamic MRI. Magnetic Resonance in Medicine. 2008;**59**(2):365-373

[45] Lustig M, Donoho D, Pauly JM. Sparse MRI: The application of compressed sensing for rapid MR imaging. Magnetic Resonance in Medicine. 2007;**58**(6):1182-1195

[46] Donoho DL. Compressed sensing. IEEE Transactions on Information Theory. 2006;**52**(4):1289-1306

[47] Block KT, Uecker M, Frahm J. Undersampled radial MRI with multiple coils. Iterative image reconstruction using a total variation constraint. Magnetic Resonance in Medicine. 2007;**57**(6):1086-1098

[48] Knoll F et al. Second order total generalized variation (TGV) for MRI. Magnetic Resonance in Medicine. 2011;**65**(2):480-491

[49] Ying L, Xu D, Liang Z-P. On Tikhonov regularization for image reconstruction in parallel MRI. In: Engineering in Medicine and Biology Society, 2004. IEMBS'04. 26th Annual International Conference of the IEEE. IEEE; 2004

[50] Daubechies I, Defrise M, De Mol C. An iterative thresholding algorithm for linear inverse problems with a sparsity constraint. Communications on Pure and Applied Mathematics. 2004;**57**(11):1413-1457

[51] Wang C et al. Accelerated brain DCE-MRI using iterative reconstruction with total generalized variation penalty for quantitative pharmacokinetic analysis: A feasibility study. Technology in Cancer Research & Treatment. 2017;**16**(4):446-460

[52] Subashi E et al. A comparison of radial keyhole strategies for high spatial and temporal resolution 4D contrast-enhanced MRI in small animal tumor models. Medical Physics. 2013;**40**(2):022304

[53] Brock KK, Consortium DRA. Results of a multi-institution deformable registration accuracy study (MIDRAS). International Journal of Radiation Oncology, Biology, Physics. 2010;**76**(2):583-596

[54] Yang J et al. Four-dimensional magnetic resonance imaging using axial body area as respiratory surrogate: Initial patient results. International Journal of Radiation Oncology, Biology, Physics. 2014;**88**(4):907-912

[55] Stemkens B et al. Image-driven, model-based 3D abdominal motion estimation for MR-guided radiotherapy. Physics in Medicine & Biology. 2016;**61**(14):5335

[56] Harris W et al. A technique for generating volumetric cine-magnetic resonance imaging. International Journal of Radiation Oncology, Biology, Physics. 2016;**95**(2):844-853

[57] Wang C et al. TU-AB-BRA-09: A novel method of generating ultrafast volumetric cine MRI (VC-MRI) using prior 4D-MRI and on-board phase-skipped encoding acquisition for radiotherapy target localization. Medical Physics. 2016;**43**(6Part33):3735-3735

[58] Wang C et al. A novel method of generating onboard 4D-MRI for liver SBRT target localization using prior 4D-MRI simulation and onboard limited angle kV acquisition from a conventional LINAC. International Journal of Radiation Oncology Biology Physics. 2017;**99**(2):S126-S127

[59] Harris W et al. A novel method to generate on-board 4D MRI using prior 4D MRI and on-board kV projections from a conventional LINAC for target localization in liver SBRT. Medical Physics. 2018;**45**(7):3238-3245

[60] Li G et al. Introduction of a pseudo demons force to enhance deformation range for robust reconstruction of super-resolution time-resolved 4 DMRI. Medical Physics. 2018;**45**(11):5197-5207

[61] Thompson RF et al. Artificial intelligence in radiation oncology imaging. International Journal of Radiation Oncology Biology Physics. 2018;**102**(4):1159-1161

[62] Oar A et al. Comparison of four dimensional computed tomography and magnetic resonance imaging in abdominal radiotherapy planning. Physics and Imaging in Radiation Oncology. 2018;**7**:70-75

[63] Lagendijk JJ, Raaymakers BW, Van Vulpen M. The magnetic resonance imaging–linac system. Seminars in Radiation Oncology. Philadelphia, PA: WB Saunders; 2014;**24**(3)

[64] Han F et al. Respiratory motion-resolved, self-gated 4D-MRI using rotating Cartesian K-space (ROCK): Initial clinical experience on an MRI-guided radiotherapy system. Radiotherapy and Oncology. 2018;**127**(3):467-473